


Thermal bias induced charge current in a Josephson junction: From ballistic to disorderedAabir Mukhopadhyay^{✉*} and Sourin Das^{✉†}*Indian Institute of Science Education & Research Kolkata, Mohanpur, Nadia 741246, West Bengal, India* (Received 10 December 2021; revised 12 July 2022; accepted 3 August 2022; published 22 August 2022)

It is known that Josephson junction (JJ) hosting scattering centers with energy-dependent scattering amplitudes, which breaks the $\omega \rightarrow -\omega$ symmetry (where ω is the excitation energy of electron about the Fermi level) exhibits finite thermoelectric response. In contrast, here we show that even in a ballistic JJ this symmetry is broken and it leads to a nonzero thermal-bias induced charge current above the gap, when the junction length is of the order of coherence length of the superconductor and the corresponding response confirms to the universal sinusoidal dependence on ϕ_{12} , where ϕ_{12} is the superconducting phase bias. In presence of multiple scatterers in the junction region, we have numerically shown that the sign of the even-in- ϕ_{12} part of the this response fluctuates violently from one disorder configuration to another hence averaging to vanishingly small values while the odd part tends towards the universal sinusoidal dependence on ϕ_{12} as we approach the large disorder limit under disorder averaging.

DOI: [10.1103/PhysRevB.106.075421](https://doi.org/10.1103/PhysRevB.106.075421)**I. INTRODUCTION**

Thermoelectric response of a hybrid junction between two normal metals in the mesoscopic regime has been discussed extensively both theoretically and experimentally [1–15]. Analogous situation comprising of a junction of superconductors is a less explored topic although discussion of thermoelectric response of superconductor has a long history. Such set-ups are of great importance because of the possibility of their applications in improving the efficiency of thermoelectric generator by strongly suppressing Ohmic losses [16–21].

In 1944, Ginzberg [22,23] showed that a temperature gradient in a bulk superconductor leads to a finite normal current response, although this current gets completely canceled by a counter flow of supercurrent in a homogeneous isotropic superconductor, which makes it impossible to detect the thermoelectric response in isolation. This fact led him to theoretically explore the possibilities of anisotropic and inhomogeneous superconductor for the detection of the thermoelectric effect. Since then, various theoretical studies [24–29] has been conducted exploring possibilities of detection of thermoelectric response of superconductors in anisotropic and inhomogeneous situations. Experimental study in this direction goes back all the way to 1920s [30–38] and this topic has been revisited in the recent past in an interesting paper by Shelly *et al.* [39]. The discovery of Josephson effect [40] in 1962 provided a natural setting for exploring thermoelectric response for a inhomogeneous superconductor. Later in 1997, Guttman and Bergman made an attempt to theoretically explore the thermoelectric response of a Josephson junction (JJ) in a tunnel Hamiltonian approach [41].

Pershoguba and Glazman [42] have carried out an elaborate study on the possibility of generating thermometric current across a junction between two quasi-one-dimensional superconductors, which goes beyond the tunneling limit and also discussed the relevance of the odd and the even part of the Josephson current as a function of the superconducting phase bias ϕ_{12} owing to scattering in junction region, which breaks the $\omega \rightarrow -\omega$ symmetry. In this regard, the helical edge state of two dimensional topological insulators pose an interesting and clean testing ground for such theoretical study, which hosts one-dimensional Josephson junction [43]. It should be noted, the constraint that the $\omega \rightarrow -\omega$ symmetry (sometimes also referred to as particle-hole symmetry) needs to be broken for inducing a finite thermoelectric response is valid only within the linear response limit, and no more holds in the nonlinear regime [44,45].

Thermal response of quantum Hall edge has already been studied in experiment [46] and hence a similar experimental set-up involving the spin Hall edge may not be far in the future. Recent theoretical studies have explored the possibility of inducing thermoelectric effect in helical edge state-based Josephson junction involving either an anisotropic ferromagnetic barrier [47,48] or a three-terminal geometry [49–51]. In this paper we study a linear response coefficient, defined as the thermal-bias induced charge current per unit temperature gradient flowing above the superconducting gap solely due to application of a thermal bias across a Josephson junction, which we refer to as “thermocurrent coefficient” and we refrain from calling it a conventional thermoelectric effect due to subtle difference between the two, which will be discussed later. We show that the thermocurrent effect can exist in the helical edge state (HES) of quantum spin Hall (QSH) insulator even in a simplest case of two terminal ballistic JJ owing to breaking of the $\omega \rightarrow -\omega$ symmetry of the quasiparticle transmission probabilities across the junction at finite length. We argue that this is generic to ballistic JJ and is not specific to HES. Lastly,

*aabir.riku@gmail.com

†sourin@iiserkol.ac.in

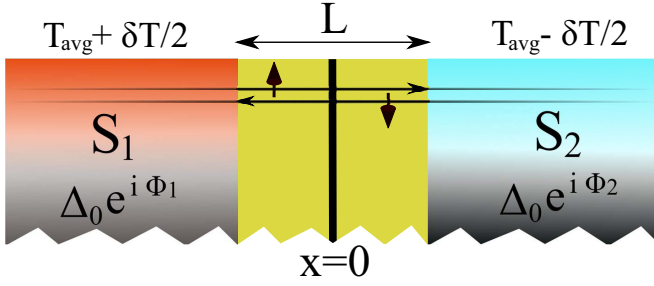


FIG. 1. Schematic of a finite-length Josephson junction set-up based on helical edge state of a 2D quantum spin Hall insulator. Superconducting leads (S_1 and S_2) are kept at different temperatures. Also there is a superconducting phase bias between S_1 and S_2 . The up and down arrows indicate the direction of spin-polarization of the corresponding edge states.

it is worth noting that the use of thermal transport for probing quantum states has been much in pursuit in contemporary science [52] and hence such a discussion is quite timely.

The paper is organized as follows. In Sec. II we described the JJ based on HES of a 2D QSH state and in Sec. III we discussed how a long ballistic JJ can break the $\omega \rightarrow -\omega$ symmetry and hence resulting in thermocurrent response, which also survives in presence of disorder. In Sec. IV we extend our discussion to the odd-in- ϕ_{12} and even-in- ϕ_{12} part of the and shown that minimal breaking of the $\omega \rightarrow -\omega$ symmetry is not enough to induce an even-in- ϕ_{12} contribution. We have also argued that the presence of thermoelectric response through the breaking of $\omega \rightarrow -\omega$ symmetry is not unique to HES, rather it is a generic property of a JJ.

II. BALLISTIC JOSEPHSON JUNCTION IN HELICAL EDGE STATE

We first consider a JJ based on 1D Dirac fermions in proximity to a s -wave superconductor, realized in a HES of QSH insulator [53–55] because of its algebraic simplicity. Later we will also explore the case of quadratic dispersion. The junction is considered to be of length L laying over the region $|x| < L/2$. The proximitized region of the edge are described by the Bogoliubov-de Gennes (BdG) Hamiltonian in the Nambu basis [53,54] ($(\psi_\uparrow, \psi_\downarrow), (\psi_\downarrow^\dagger, -\psi_\uparrow^\dagger)$) as

$$\mathcal{H} = (-i\hbar v_F \partial_x \sigma_z - \mu) \tau_z + \Delta(x) (\cos \phi_r \tau_x - \sin \phi_r \tau_y), \quad (1)$$

where σ and τ are the Pauli matrices representing spin and particle-hole degrees of freedom respectively. The superconducting pairing potential is given by $\Delta(x) = \Delta_0 [\Theta(-x - L/2) + \theta(x - L/2)]$ such that it defines a superconductor-normal-superconductor junction (SNS). Superconducting leads (S_r) are identified as $r \in \{1, 2\}$ (left lead being $r = 1$ and the right being $r = 2$) and ϕ_r are the corresponding superconducting phases (see Fig. 1); μ is the chemical potential throughout the edge and v_F is the corresponding Fermi velocity. We also consider the doping (i.e., the value of chemical potential μ) to be finite ($\mu \neq 0$) and the length of the junction L to be comparable to the superconducting coherence length $\xi = \hbar v_F / \Delta_0$ such that $(p_e - p_h)L/\hbar$ can be of the order of unity for energies $\leq \Delta_0$, where $p_{e,h} = \hbar k_{e,h}$ are

the quasiparticle and the corresponding quasihole momenta for particles in the junction region. Note that, in general, for highly doped superconductor with quadratic dispersion $p_e \approx p_h$ and hence such phases are generally neglected. On the other hand, if such phase accumulation becomes of the order of unity, it naturally leads to breaking of $\omega \rightarrow -\omega$ symmetry of the excited Bogoliubov quasielectron and quasihole transmission probabilities individually across the junction leading to finite thermocurrent effect, although the sum of the two does respect the symmetry.

III. $\omega \rightarrow -\omega$ SYMMETRY BREAKING AND ANDREEV BOUND STATE OF BALLISTIC JOSEPHSON JUNCTION

Let us consider a right moving electron-like quasiparticle, which starts its journey at $x = -L/2$ and propagates through the normal region and reaches at $x = L/2$. It Andreev reflects back as a hole with an unimodular amplitude by creating a Cooper pair in the superconducting lead 2 (S_2). The reflected hole then travels through the normal region and reaches back to $x = -L/2$. It then suffers a second Andreev reflection hence annihilating a Cooper pair at superconducting lead 1 (S_1) and completing a closed loop journey resulting in shuttling of a single Cooper pair from S_1 to S_2 [see Fig. 2(a)]. This process involving a right-moving electron and a left-moving hole can be directly related to formation of a Andreev bound state (ABS) at the JJ where the ABS energy is given by $\omega_0^{21} = \pm \Delta_0 |\cos(\frac{k_e(\omega_0^{21}) - k_h(\omega_0^{21})}{2} L - \frac{\phi_{12}}{2})|$ where $\phi_{12} = \phi_2 - \phi_1$ and $k_{e,h}(\omega_0) = (\mu \pm \omega_0)/(\hbar v_F)$ (see Appendix B). Similarly, if a right-moving hole-like quasiparticle starts from $x = -L/2$ and completes the cycle after two Andreev reflections, it will transfer a Cooper pair from S_2 to S_1 [see Fig. 2(a)] and the corresponding ABS will be formed at energies $\omega_0^{12} = \pm \Delta_0 |\cos(\frac{k_e(\omega_0^{12}) - k_h(\omega_0^{12})}{2} L + \frac{\phi_{12}}{2})|$ (see Appendix B). Note that the ω_0^{21} and ω_0^{12} transform into one another as $\phi_{12} \rightarrow -\phi_{12}$. The ABS energies ω_0^{21} and ω_0^{12} are shown as a function of ϕ_{12} for different values of the junction length L in Fig. 2(b). The important point to note here is the fact that, for finite L , the degeneracy between ω_0^{21} and ω_0^{12} is lifted whenever $\phi_{12} \neq 0, \pi$ and this fact leads to an asymmetry between the transmission probability of electron (hole)-like BdG quasiparticle above the gap, incident on the junction from the left and right hence leading to finite thermocurrent response. Also, it should be noted that the ABS energies are defined through self-consistent transcendental equations, leading to a possibility of having a multivalued solutions, such as for $L = 2\xi$ in Fig. 2(b) and the solutions are independent of the value of μ owing to linear dispersion.

Now, for analyzing the implication of degeneracy lifting of ABS on the thermocurrent effect of the junction, we start by calculating the scattering amplitude for Bogoliubov quasiparticle above the gap ($\omega > \Delta_0$) across the JJ. It is straightforward to match the plane wave solutions of the BdG equation to obtain the transmission probabilities across the JJ (from S_1 to S_2) as described by Eq. (1) are given by (see Appendix B)

$$\mathcal{T}_{ee}^{21} = \mathcal{T}_{hh}^{12} = \frac{\omega^2 - \Delta_0^2}{\omega^2 - \Delta_0^2 \cos^2(\frac{k_e - k_h}{2} L - \frac{\phi_{12}}{2})}, \quad (2)$$

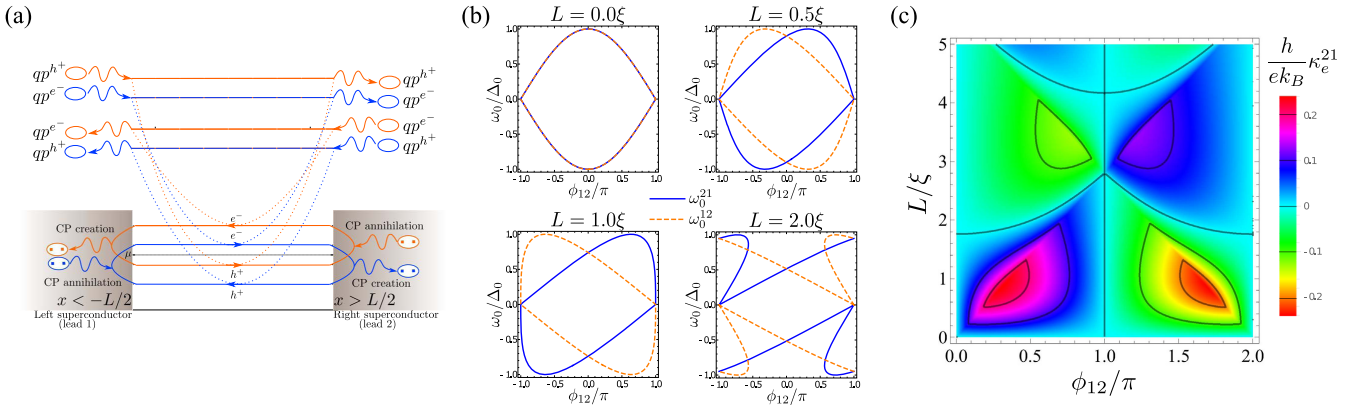


FIG. 2. (a) Pictorial representation of below the gap ($\omega < \Delta_0$) tunneling of Cooper pairs (CP) from left (right) to right (left) via two different Andreev bound states ω_0^{21} (indicated by blue lines) and ω_0^{12} (indicated by orange lines). The dotted lines represent the fact that tunneling of the quasielectrons (quasiholes) above the gap ($\omega > \Delta_0$) across the junction are in correspondence with distinct bound states, as can be noted from the poles of the quasielectron (quasihole) transmission probabilities \mathcal{T}_{ee}^{21} and \mathcal{T}_{ee}^{12} (or \mathcal{T}_{hh}^{12} and \mathcal{T}_{hh}^{21}). (b) Two types of Andreev bound states as a function of superconducting phase difference ϕ_{12} are plotted for different values of junction lengths where $\xi = \hbar v_F / \Delta_0$ is the superconducting coherence length. (c) Density plot for the thermocurrent coefficient κ_e^{21} of a ballistic JJ based on the edge states of a quantum spin Hall insulator in proximity to a s -wave superconductor, as a function of superconducting phase bias ϕ_{12} and junction length L . The average temperature of the junction is considered to be $k_B T_{\text{avg}} = 0.56\Delta_0$ where the effective superconducting gap at this temperature is taken to be $\Delta_{T_{\text{avg}}} \sim 0.56\Delta_0$. Both the plots (b) and (c) are valid for any value of the chemical potential μ .

$$\mathcal{T}_{hh}^{21} = \mathcal{T}_{ee}^{12} = \frac{\omega^2 - \Delta_0^2}{\omega^2 - \Delta_0^2 \cos^2\left(\frac{k_e - k_h}{2}L + \frac{\phi_{12}}{2}\right)}, \quad (3)$$

while $\mathcal{T}_{he}^{21} = \mathcal{T}_{eh}^{21} = \mathcal{T}_{he}^{12} = \mathcal{T}_{eh}^{12} = 0$. Quasiparticle transmission probabilities through a ballistic JJ is shown in Fig. 3 for two different lengths of the junction. Here $\mathcal{T}_{q'q}^{ji}$ denote the transmission probability of a q -like QP ($q = e, h$) from lead S_i to a q' -like QP in lead S_j . Note that the tunneling of an electron (hole)-like QP from S_1 to S_2 (S_2 to S_1) is in correspondence with the ABS having energy ω_0^{21} while the tunneling of a hole (electron)-like QP from S_1 to S_2 (S_2 to S_1) is in correspondence with the ABS having energy ω_0^{12} [see Fig. 2(a)], which is apparent from the fact that the poles of the transmission amplitudes for these two processes coincides

with the corresponding ABS energies. Within linear response theory, thermocurrent coefficient of a JJ can be defined in terms of the transmission probabilities as [42]

$$\kappa_e^{21} = \left[\frac{e}{\hbar} \int_{\Delta}^{\infty} d\omega \frac{\omega}{\sqrt{\omega^2 - \Delta^2}} [i_e^{21} - i_h^{21}] \frac{df(\omega, T)}{dT} \right]_{T=T_{\text{avg}}} \quad (4)$$

where $i_e^{21} = (\mathcal{T}_{ee}^{21} - \mathcal{T}_{he}^{21})$, $i_h^{21} = (\mathcal{T}_{hh}^{21} - \mathcal{T}_{eh}^{21})$, e is the electronic charge, $f(\omega, T)$ is the Fermi distribution function at temperature T , $df(\omega, T)/dT = \omega \text{sech}^2(\omega/(2k_B T))/(4k_B T^2)$, and T_{avg} is the average temperature of the junction. Note that, in the limit $L \rightarrow 0$, κ_e^{21} is zero.

The integration in Eq. (4) can be done numerically and κ_e^{21} can be obtained as a function of superconducting phase

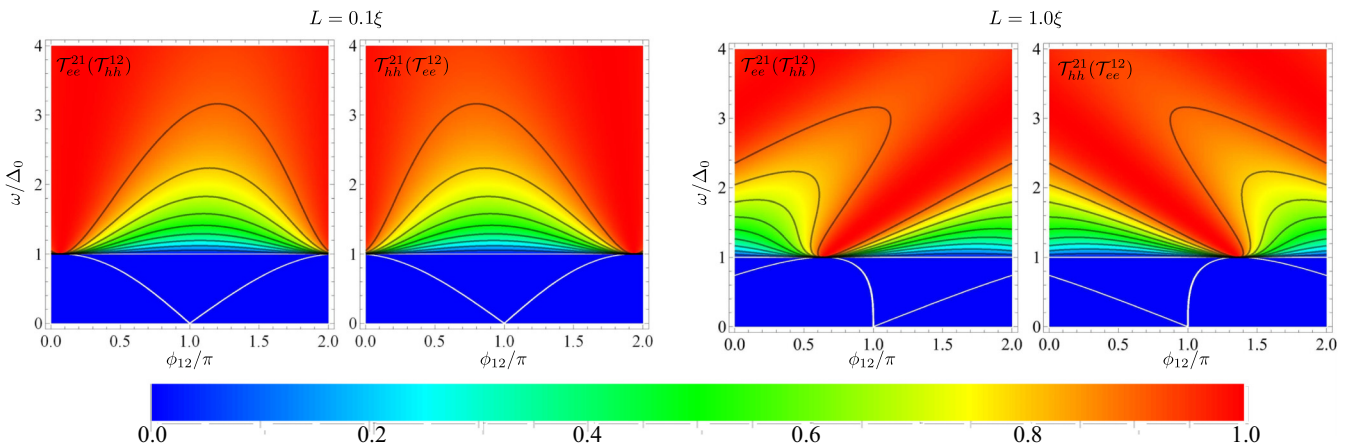


FIG. 3. Different transmission probabilities of the quasiparticles through a ballistic Josephson junction based on the helical edge state of a quantum spin Hall insulator, in the space of energy (ω) and superconducting phase difference (ϕ_{12}) for different values of junction length (L). A clear asymmetry between the electron and hole transmission probability from left (right) to right (left) develops as we increase the length of the junction. The plot in energy window ($|\omega| < \Delta_0$) signifies the evolution of the pole (location of Andreev bound states) of the transmission amplitude as a function of ϕ_{12} . The plots are valid for any value of the chemical potential μ .

difference ϕ_{12} and junction length L , which is plotted as a density plot in Fig. 2(c). In case of HES, owing to its linear dispersion, the value of the overall chemical potential μ does not effect the calculations for the ballistic case.

To obtain an estimate of the extremum values of thermocurrent coefficient for a single channel ballistic junction, we perform a numerical scan over the parameter space of ϕ_{12} and L for a given temperature of $k_B T_{\text{avg}} = 0.5\Delta_0$. It is important to note that, if the average temperature T_{avg} is comparable to the critical temperature of the superconductor (T_C), then the temperature dependence of the superconducting gap should be taken into consideration and the value of the superconducting pairing potential has to be modified accordingly. At temperature $T_{\text{avg}} = 0.5\Delta_0/k_B$, BCS theory (Berdeen-Cooper-Schrieffer theory) predicts $\Delta_{T_{\text{avg}}} \sim 0.56\Delta_0$ [56,57]. After taking this into consideration we found that the maximum of (minimum of) $|\kappa_e^{21}| \approx 0.241391 ek_B/h$ ($\approx 0.8nA/K$), obtained for a junction length of $L \approx 0.861\xi$ for $\phi_{12} \approx 0.307\pi$ (minimum at $\phi_{12} \approx 1.693\pi$). It is important to note that this maximum value of the thermocurrent coefficient is much larger than some of the existing experimentally measured values in the context of thermoelectric materials [58] or some of the theoretical predictions in the context of Andreev interferometers [51]. This value is obtained by simultaneously optimizing the superconducting phase difference ϕ_{12} , opacity of the junction τ , and length of the junction L . Moreover, a number of assumptions have been considered, e.g., (i) liner response limit is valid, (ii) the bandwidth of the edge state is large enough such that at the given temperature, the edge state remains robust and do not hybridize with the bulk of the 2D QSH insulator, and (iii) the bandwidth of the edge state is much larger than the superconducting gap.

As we can see from Fig. 3, for a ballistic JJ, in general for any given value of ϕ_{12} and at an energy $\omega > \Delta_0$ the quasipar-

ticle transmission probabilities \mathcal{T}_{ee}^{21} and \mathcal{T}_{hh}^{21} are different if the length of the junction L is comparable to the superconducting coherence length (i.e., when we are not in the short junction limit). Note that the difference between these quantities at a given ω is maximum in the neighborhood of $\omega = \Delta_0$ and it decreases as we go higher in ω , although nonmonotonically. Additionally, one must notice that the thermocurrent effect identically vanishes both at $\phi_{12} = 0$ and π , which are the time reversal symmetric points [see Fig. 2(c)].

IV. EVEN-IN- ϕ_{12} AND ODD-IN- ϕ_{12} PART OF THE THERMOCURRENT RESPONSE AND THE EFFECT OF DISORDER

Presence of scatter within the junction region, which breaks the $\omega \rightarrow -\omega$ symmetry, not only leads to a finite thermo-current effect, but also results in deviation from thermocurrent coefficient being odd in ϕ_{12} [42]. As discussed above, a JJ of finite length also breaks the $\omega \rightarrow -\omega$ symmetry hence it is curious if this minimal symmetry breaking can result in such a deviation, i.e., the thermocurrent response can be written as a liner sum of an even-in- ϕ_{12} part and an odd-in- ϕ_{12} part.

It is straightforward to check that the expression for thermocurrent coefficient in the ballistic limit, obtained from Eqs. (2)–(4) is an odd function of ϕ_{12} , independent of the length of the junction. This implies that the breaking of $\omega \rightarrow -\omega$ symmetry via $k_e \neq k_h$ (as discussed in the previous section) does not lead to any contribution to the thermocurrent response, which is even in ϕ_{12} . Further, we calculate the thermocurrent coefficient in presence of a single localized scatterer, which is positioned at an arbitrary point within the junction region and we assume that the scattering matrix corresponding to the scatterer has no energy dependence. The expression for the thermocurrent coefficient in this case is given below,

$$\kappa_e^{21} = \left[\frac{e}{h} \int_{\Delta}^{\infty} d\omega \frac{\omega}{\sqrt{\omega^2 - \Delta^2}} \left[\frac{4\tau((1-\tau)\sin((k_e - k_h)L(m-n)) + \sin((k_e - k_h)L)) \sin\phi_{12} \sinh 2\theta}{\Omega\Omega^*} \right] \frac{df(\omega, T)}{dT} \right]_{T=T_{\text{avg}}}, \quad (5)$$

where, $\Omega = (1-\tau)\cos((k_e - k_h)L(m-n)) + \cos((k_e - k_h)L - 2i\theta) - \tau\cos\phi_{12}$, $\theta = \text{arccosh}\omega/\Delta_0$, τ is the normal state transmission probability across the scatterer and the position of the scattering center divides the junction region in the ratio $m:n$ ($m, n \leq 1$ and $m+n=1$). All other notations have their usual meanings as discussed before. Equation (5) clearly shows that the thermocurrent response, in this case also, is odd in ϕ_{12} . Hence, our study establishes the fact that the minimal breaking of $\omega \rightarrow -\omega$ symmetry for a finite length ballistic junction (or in presence of a single scatterer, which does not break the $\omega \rightarrow -\omega$ symmetry) is sufficient to induce thermocurrent response across the JJ, although it is not enough to induce an even-in- ϕ_{12} contribution to the thermocurrent coefficient.

Now, if we consider a situation comprising of more than one such scatterer, then the effective scattering matrix describing the collection of scatterers will become energy dependent

and in general will also break the $\omega \rightarrow -\omega$ symmetry, resulting in an even-in- ϕ_{12} contribution to the thermocurrent coefficient as expected [42]. The even-in- ϕ_{12} part of the thermocurrent coefficient is proportional to $(\tau_{\omega} - \tau_{-\omega})$, where τ_{ω} is the normal state transmission probability across the junction at an energy ω , and thus can vary drastically (both in amplitude and in sign) for different disorder configurations for a given ϕ_{12} . Hence, averaging over random configurations results in vanishingly small values of the even part. Next we perform a numerical calculation to analyze the effect of averaging over a large number of disorder configurations in presence of multiple scatterers. To begin with, we consider four scattering centers represented by four energy-independent scattering matrices placed at random positions inside the junction region. Transmission probabilities of the scattering matrices are chosen randomly from a one-sided Gaussian distribution with a mean of 95% and standard

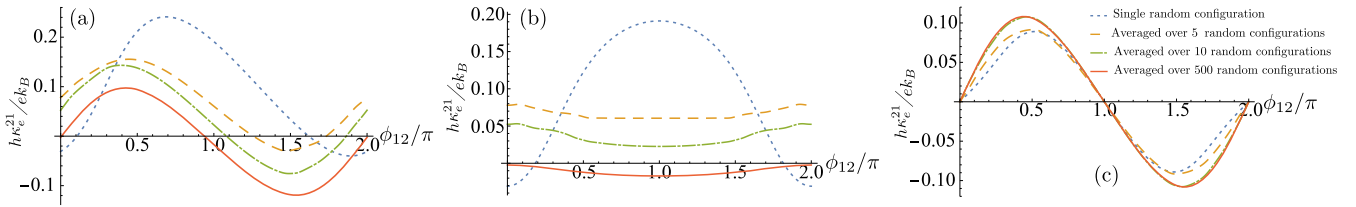


FIG. 4. Thermocurrent coefficient of a Josephson junction based on helical edge state of quantum spin Hall insulator in presence of four random scattering centers. (a) Total thermocurrent coefficient (b) the part of thermal conductance that is even in ϕ_{12} (c) the part of conductance that is odd in ϕ_{12} , for single random configuration of scattering centers and after averaging over different numbers of random configurations. The average temperature of the junction is considered to be $k_B T_{\text{avg}} = 0.5\Delta_0$, where the effective superconducting gap at this temperature is taken to be $\Delta_{T_{\text{avg}}} \sim 0.56\Delta_0$, and the overall chemical potential to be $\mu = 10\Delta_0$. Length of the junction is considered to be $L = 0.87\xi$ where ξ is the superconducting coherence length.

deviation of 5%. All the phase freedom of the disorders have been chosen randomly from a Gaussian distribution with a mean of 0 and standard deviation 0.05π . We have fixed the length of the junction to be $L \sim 0.87\xi$, the value at which we get maximum thermocurrent coefficient (which occurs for $\phi \sim 0.31\pi$) for a ballistic JJ. It can be seen clearly from Fig. 4 that averaging over as-small-as 10 configurations already shows a convergence towards an odd-in- ϕ_{12} behavior while the even-in- ϕ_{12} part is strongly suppressed. It is interesting to note that, in absence of an averaging (corresponding to a fixed quenched disorder configuration), for certain range of values of ϕ_{12} , the even part can be the dominant contribution in the net thermocurrent coefficient (see Fig. 4).

Now we extend the numerical analysis to a larger number of scattering centers. The scattering centers are modeled as before and the length of the junction is fixed at $L = 0.87\xi$. For a given number of scattering centers, disorder average is done over 500 configurations where we have checked that beyond this, there is negligible variation of the result. The mean and the variance of the thermocurrent coefficients are plotted as a function of the superconducting phase difference ϕ_{12} in Fig. 5. Note that, in presence of a single scatterer, the variance of the thermocurrent coefficient is smallest because in this case there is no even-in- ϕ_{12} part of the thermocurrent coefficient. We have also observed that, in general, the variance is relatively lower in the neighborhood of $\phi_{12} = \pi$ rather than in the neighborhood of $\phi_{12} = 0$ or 2π . To conclude, the plot for thermocurrent coefficient after averaging tend to reduce to

the universal sinusoidal dependence of ϕ_{12} as the number of scatterers within the junction region increases (see the middle panel of Fig. 5). This is due to the fact that, with increasing opacity of the JJ, the ϕ_{12} sensitivity of the thermocurrent coefficients via the poles of the quasiparticle transmission probabilities decreases and the major contribution comes from the explicit $\sin(\phi_{12})$ factor in the numerator.

V. DISCUSSION

Occurrence of thermocurrent effect through the breaking of $\omega \rightarrow -\omega$ symmetry for a ballistic long JJ is not specific to the HES. 1D JJ with quadratic dispersion and with s -wave or p -wave superconductivity should also demonstrate such a response. Of course, in the high doping limit, the thermocurrent coefficient should reduce to the results obtained in the paper when linearized about the Fermi energy. Thus, the thermocurrent response is a generic property of any ballistic JJ with junction length of the order of the superconducting coherence length. However, with the increasing opacity of the JJ for junction length less than the superconducting coherence length, the ABS energies tend to move towards the zero energy for p -wave superconductivity due to the presence of Majorana fermions. Whereas, for a JJ with s -wave superconductivity within the same limit, the ABS energies tend to move towards the continuum with increasing opacity of the junction. This fact manifests itself in the thermocurrent coefficient via the poles of the quasiparticle transmission probabilities. Also,

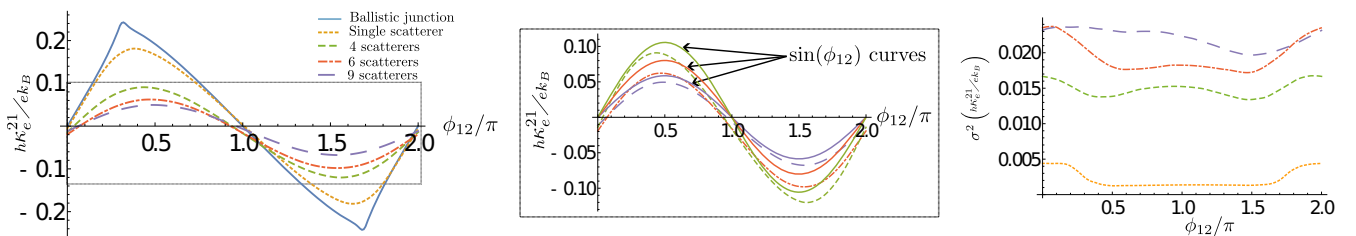


FIG. 5. Disordered averaged mean value (left) and the variance (right) of the thermocurrent coefficient κ_e^{21} of a Josephson junction based on the helical edge states of a quantum spin Hall insulator with proximity to a s -wave superconductor, are plotted as a function of superconducting phase difference ϕ_{12} . The average temperature of the junction is considered to be $k_B T_{\text{avg}} = 0.5\Delta_0$, where the effective superconducting gap at this temperature is taken to be $\Delta_{T_{\text{avg}}} \sim 0.56\Delta_0$, and the overall chemical potential to be $\mu = 10\Delta_0$. Length of the junction is considered to be $L = 0.87\xi$ where ξ is the superconducting coherence length. Average is done over 500 disorder configurations. The middle plot shows that, as we increase the number of scatterers, the curves for thermocurrent coefficients tend to a $\sin(\phi_{12})$ curves (solid lines) with an amplitude $(\max(\kappa_e^{12}) - \min(\kappa_e^{21}))/2$.

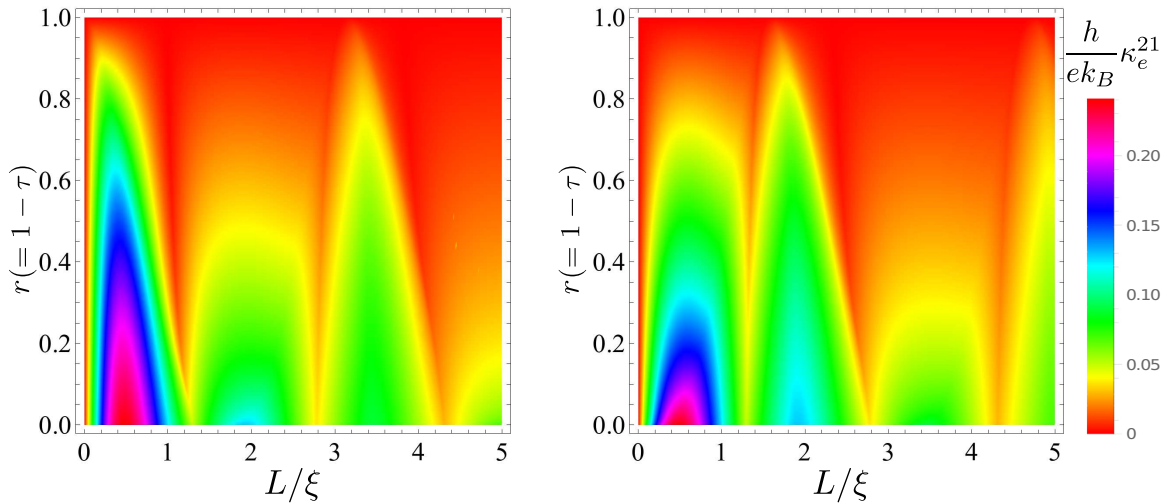


FIG. 6. The maximum possible thermocurrent coefficient of a JJ with (left) s -wave and (right) p -wave superconductivity for a given junction length and normal state reflection probability r (as calculated with the analytic approximation $\mu \gg \Delta_0, k_B T$). Note that the scatterer is assumed to be energy independent and is placed at the middle of the junction. The parameters are assumed to be $\mu = 100\Delta_0$ and $k_B T_{\text{avg}} = 0.5\Delta_0$ where the effective superconducting gap at this temperature is taken to be $\Delta_{T_{\text{avg}}} \sim 0.56\Delta_0$.

for JJ with junction length longer than the superconducting coherence length, the states from the continuum spectrum tend to leak into the superconducting gap, thereby changing the details of the thermocurrent coefficient.

Further, to check if the s -wave or the p -wave leads to a larger thermocurrent coefficient for a given junction length we perform an analysis where we have placed an energy-independent scatterer at the middle of a JJ, and plotted the maximum possible thermocurrent coefficient (scanned over all values of ϕ_{12}) for a given junction length L and given transparency of the scatterer (normal state transmission probability τ) as shown in Fig. 6. We have performed this study within the approximation $\mu \gg \Delta_0, k_B T$ (see Appendix D and Appendix E). From these results we can conclude that in general, there is no distinguishable pattern in the thermocurrent coefficient for the case of s -wave and p -wave superconductivity.

Lastly we want to mention that in general, the transport phenomenon, which is happening above the gap is expected to be purely dissipative and hence may be related to entropy generation. On the other hand we should note that the quasiparticle excitations of the BdG equation are good eigenstates of the system asymptotically away from the junction but in the junction area they are no more good eigenstates and hence lead to coherent mixing (interference) between the scattering states above the gap and the Andreev bound states inside the gap. It is straightforward to identify such an interference term in the weak tunneling limit of the Josephson junction, as discussed in Ref. [41] (and in Refs. [59–61]), where it is shown that the total current I_{tot} due to thermal bias can be written as a sum of normal current of quasiparticles tunneling (I_{qp}), the quasiparticle-pair interference current ($I_{qp\text{-}pair}$) and the nondissipative Josephson pair current (I_{pair}) i.e., $I_{\text{tot}} = I_{qp} + I_{qp\text{-}pair} + I_{\text{pair}}$. Presence of such an interference term is the reason behind the obstruction to the clear identification of a conventional thermoelectric coefficient and its connection to entropy generation in the case of a Josephson junction.

This situation gets even worse in the strong coupling limit or the ballistic limit (which is exactly opposite to the tunneling limit) where such interference terms are expected to have larger contributions to the current. This fact motivated us to define and study the thermocurrent coefficient rather than a conventional thermoelectric coefficient in this paper.

As far as the possible strategy for the measurement of the thermocurrent current is concerned, it cannot be measured in isolation as it will always be accompanied by the finite temperature Josephson current. However, there may be ways to measure the thermocurrent coefficient indirectly. For example, consider a situation where a JJ is initially maintained at an equilibrium temperature T . The current that is obtained, is totally the Josephson current $S_{(T,T)} = I_J$, where the first (second) subscript corresponds to the temperature of the left (right) lead S_1 (S_2). Now, if S_1 is raised to temperature $T + \delta T$, then the corresponding total current will be a sum of the Josephson current and the thermocurrent $S_{(T+\delta T,T)} = I_J - \delta I_J + \kappa_e^{21} \delta T$, where δI_J is the variation in the Josephson current due temperature bias. Next, consider the situation where S_1 is kept at temperature T while S_2 is raised to temperature $T + \delta T$, then the corresponding total current will be $S_{(T,T+\delta T)} = I_J - \delta I_J - \kappa_e^{21} \delta T$. Now if, $(2S_{(T,T)} - (S_{(T+\delta T,T)} + S_{(T,T+\delta T)}))/2S_{(T,T)} \ll 1$ then a measurement of the ratio $(S_{(T+\delta T,T)} - S_{(T,T+\delta T)})/2\delta T$ will provide the thermocurrent coefficient. Note that a similar strategy involving $\phi_{12} \rightarrow -\phi_{12}$ rather than involving $\delta T \rightarrow -\delta T$ is difficult to implement due to the presence of even-in- ϕ_{12} part of the thermocurrent coefficient.

ACKNOWLEDGMENTS

A.M. thanks Vivekananda Adak for helpful discussions. We thank Chris Olund, Sergey Pershoguba, and Erhai Zhao for useful communication over email. A.M. acknowledges Ministry of Education, India for funding. S.D. would like to acknowledge the MATRICS Grant (No. MTR/2019/001 043)

from the Science and Engineering Research Board (SERB), India for funding.

APPENDIX A: MATRIX FORMALISM

To have a clear physical insight into different semiclassical paths that give rise to degeneracy-lifted ABS and the thermocurrent response of a JJ, we shall be using the matrix method as discussed by Kundu *et al.* [60].

Let $\Psi_{qp[N]}^{e+(-)}$ and $\Psi_{qp[N]}^{h+(-)}$ denote forward (backward) moving electron-like QP and forward (backward) moving hole-like QP respectively within the superconducting lead S_i having superconducting phase ϕ_i ($i \in \{1, 2\}$) [within the normal region]. These wave functions can be explicitly calculated using the BdG Hamiltonian (1) in the main text or the BdG

Hamiltonian with quadratic dispersion and with s -wave or p -wave superconductivity,

$$\mathcal{H}_\eta = \left(-\frac{\hbar^2}{2m} \frac{\partial^2}{\partial x^2} - \mu \right) \tau_z + \Delta^\eta(x) (\cos \phi_r \tau_x - \sin \phi_r \tau_y), \quad (\text{A1})$$

where $\Delta^\eta(x) = \Delta_0 [\Theta(-x - L/2) + \Theta(x - L/2)] f(\eta)$, $f(\eta) = (-i\partial_x/k_F)^{(1-\eta)/2}$, $\eta = \pm 1$ for s -wave and p -wave superconductivity respectively and $p_F = \hbar k_F = \sqrt{2m\mu}$ is the Fermi momentum.

We first consider two reflection matrices \mathbb{R}^γ , $\gamma \in \{1, 2\}$, which describe both Andreev and normal reflections at the normal-superconducting junctions,

$$\begin{aligned} \mathbb{R}^1 \Psi_N^{e+} &= r_{Ahe}^1 \Psi_N^{h-} + r_{Nee}^1 \Psi_N^{e-}, & \mathbb{R}^2 \Psi_N^{e-} &= r_{Ahe}^2 \Psi_N^{h+} + r_{Nee}^2 \Psi_N^{e+}, \\ \mathbb{R}^1 \Psi_N^{h-} &= r_{Aeh}^1 \Psi_N^{e+} + r_{Nhh}^1 \Psi_N^{h+}, & \mathbb{R}^2 \Psi_N^{h+} &= r_{Aeh}^2 \Psi_N^{e-} + r_{Nhh}^2 \Psi_N^{h-}, \end{aligned} \quad \mathbb{R}^1 \Psi_N^{e-} = \mathbb{R}^1 \Psi_N^{h+} = \mathbb{R}^2 \Psi_N^{e+} = \mathbb{R}^2 \Psi_N^{h-} = 0,$$

where $r_{Aqq'}^\gamma$ and $r_{Nqq'}^\gamma$ respectively describe the amplitudes of different Andreev reflections and normal reflections.

To consider the propagation of the wave functions through a length l within the normal region, we consider two propagation matrices, \mathbb{T}^γ ($\gamma \in \{1, 2\}$), such that

$$\begin{aligned} \mathbb{T}^1(l) \Psi_N^{e+}|_x &= \Psi_N^{e+}|_{x+l}, & \mathbb{T}^2(l) \Psi_N^{e-}|_x &= \Psi_N^{e-}|_{x-l}, & \mathbb{T}^1(l) \Psi_N^{e-} &= \mathbb{T}^1(l) \Psi_N^{h+} = \mathbb{T}^2(l) \Psi_N^{e+} = \mathbb{T}^2(l) \Psi_N^{h-} = 0, \\ \mathbb{T}^1(l) \Psi_N^{h-}|_x &= \Psi_N^{h-}|_{x-l}, & \mathbb{T}^2(l) \Psi_N^{h+}|_x &= \Psi_N^{h+}|_{x+l}, \end{aligned}$$

For energies above the superconducting gap, two tunneling matrices at the two boundaries $\mathbb{T}_B^{L,R}$ are defined as

$$\begin{aligned} \mathbb{T}_B^L \Psi_{qp}^{e+}[\phi_1] &= t_e \Psi_N^{e+} + t_{Ae} \Psi_N^{h+}, & \mathbb{T}_B^R \Psi_N^{e+} &= t_e^{qp} \Psi_{qp}^{e+}[\phi_2] + t_{Ae}^{qp} \Psi_{qp}^{h+}[\phi_2], & \mathbb{T}_B^L \Psi_{qp}^{e-} &= \mathbb{T}_B^L \Psi_{qp}^{h-} \\ \mathbb{T}_B^L \Psi_{qp}^{h+}[\phi_1] &= t_h \Psi_N^{h+} + t_{Ah} \Psi_N^{e+}, & \mathbb{T}_B^R \Psi_N^{h+} &= t_h^{qp} \Psi_{qp}^{h+}[\phi_2] + t_{Ah}^{qp} \Psi_{qp}^{e+}[\phi_2], & \mathbb{T}_B^R \Psi_N^{e-} &= \mathbb{T}_B^R \Psi_N^{h-} = 0. \end{aligned}$$

We also consider scattering matrices within the normal region to account for the disorders,

$$\mathcal{T}^e \begin{bmatrix} \Psi^{e+}|_{-x} \\ \Psi^{e-}|_{+x} \end{bmatrix} = \begin{bmatrix} \Psi^{e+}|_{+x} \\ \Psi^{e-}|_{-x} \end{bmatrix} \quad \mathcal{T}^h \begin{bmatrix} \Psi^{h-}|_{+x} \\ \Psi^{h+}|_{-x} \end{bmatrix} = \begin{bmatrix} \Psi^{h-}|_{-x} \\ \Psi^{h+}|_{+x} \end{bmatrix}$$

Note that the matrices \mathcal{T}^e and \mathcal{T}^h are related by the particle-hole symmetry of the corresponding BdG Hamiltonian.

Explicit expressions of the reflection matrices \mathbb{R}^γ and tunneling matrices $\mathbb{T}_B^{L,R}$ can be obtained by demanding the continuity of the wave functions across the boundaries in case of JJ based on HES or by using the following boundary conditions in case of JJ with quadratic dispersion [61]:

$$\begin{aligned} \frac{\hbar^2}{2m} \tau_z [\partial_x^{(\beta)} \Psi_S^\pm - \partial_x^{(\beta)} \Psi_N^\pm] + i\beta \left(\frac{1-\eta}{2} \right) \frac{\Delta_0}{k_F} \\ \times [\cos \phi_\pm \tau_x - \sin \phi_\pm \tau_y] \Psi_S^\pm = 0 \end{aligned} \quad (\text{A2})$$

where $\beta \in \{0, 1\}$; $\eta = 1$ for s -wave and $\eta = -1$ for p -wave superconductivity; $\phi_+ = \phi_2$ and $\phi_- = \phi_1$; Ψ_S and Ψ_N are the wave functions in the superconducting and normal regions respectively.

APPENDIX B: CLEAN JUNCTION

Andreev bound states are the result of multiple Andreev reflections. There are two ways in which Andreev bound state can be formed as discussed in the main text. We shall describe

the same processes here with the help of matrix formalism discussed in Appendix A.

(i) *Tunneling of a Cooper pair from left to right.* An electron-like quasiparticle starts at $x = -L/2$ (i.e., $\Psi_N^{e+}|_{x=-L/2}$) and propagates through the normal region and reaches at $x = L/2$ (i.e., $\Psi_N^{e+}|_{x=L/2} = \mathbb{T}^1 \Psi_N^{e+}|_{x=-L/2}$). It Andreev reflects back as a hole with unimodular amplitude r_{Ahe}^1 (i.e., $r_{Ahe}^1 \Psi_N^{h-} = \mathbb{R}_A^1 \Psi_N^{e+}$) by creating a Cooper pair in the superconducting lead 2 (S_2). The reflected hole then travels through the normal region and reaches at $x = -L/2$ (i.e., $\Psi_N^{h-}|_{x=-L/2} = \mathbb{T}^1 \Psi_N^{h-}|_{x=L/2}$). It then again Andreev reflects as an electron with unimodular amplitude r_{Aeh}^1 (i.e., $r_{Aeh}^1 \Psi_N^{e+} = \mathbb{R}_A^1 \Psi_N^{h-}$) by annihilating a Cooper pair in the superconducting lead 1 (S_1). Now for $\omega \leq \Delta_0$, matrices \mathbb{R}^γ and \mathbb{T}^γ are unitary, so it must be

$$\Psi_N^{e+}|_{x=-L/2} = (\mathbb{R}^1 \mathbb{T}^1 \mathbb{R}^1 \mathbb{T}^1) \Psi_N^{e+}|_{x=-L/2}. \quad (\text{B1})$$

The corresponding Andreev bound state energy can be obtained by solving the determinant condition

$$\det(\mathbb{I}_{4 \times 4} - \mathbb{R}^1 \mathbb{T}^1 \mathbb{R}^1 \mathbb{T}^1) = 0, \quad (\text{B2})$$

which gives the ABS energy ω_0^1 .

(ii) *Tunneling of a Cooper pair from right to left.* If a right-moving hole-like quasiparticle starts from $x = -L/2$ (i.e., $\Psi_N^{h+}|_{x=-L/2}$) and completes the cycle after two Andreev

reflections, it can transfer a Cooper pair from S_2 to S_1 ,

$$\Psi_N^{h+}|_{x=-L/2} = (\mathbb{R}^2 \mathbb{T}^2 \mathbb{R}^2 \mathbb{T}^2) \Psi_N^{h+}|_{x=L/2}. \quad (\text{B3})$$

The corresponding Andreev bound state energy can be obtained by solving the equation

$$\det(\mathbb{I}_{4 \times 4} - \mathbb{R}^2 \mathbb{T}^2 \mathbb{R}^2 \mathbb{T}^2) = 0, \quad (\text{B4})$$

which gives the ABS energy ω_0^{12} .

Now, tunneling of a quasiparticle with energy $\omega > \Delta_0$ from S_1 to S_2 can be understood in terms of the matrices \mathbb{R}^γ , \mathbb{T}^γ and $\mathbb{T}_B^{(L,R)}$.

(i) *Tunneling of an electron (hole)-like quasiparticle from left (right) to right (left)*. For a clean junction, an incident electron-like quasiparticle in S_1 (i.e., $\Psi_{qp}^{e+}[\phi_1]$) can tunnel into S_2 as a electron-like quasiparticle (i.e., $\Psi_{qp}^{e+}[\phi_2]$) either directly or by any even number of Andreev reflections. Mathematically,

$$\begin{aligned} \chi_{ee}^{21} \Psi_{qp}^{e+}[\phi_2] &= \mathbb{T}_B^R (\mathbb{T}^1 + \mathbb{T}^1 \mathbb{R}^1 \mathbb{T}^1 \mathbb{R}^1 \mathbb{T}^1 + \dots) \mathbb{T}_B^L \Psi_{qp}^{e+}[\phi_1] \\ &= \mathbb{T}_B^R \mathbb{T}^1 (\mathbb{I} - \mathbb{R}^1 \mathbb{T}^1 \mathbb{R}^1 \mathbb{T}^1)^{-1} \mathbb{T}_B^L \Psi_{qp}^{e+}[\phi_1]. \end{aligned} \quad (\text{B5})$$

It is clear from Eqs. (B5) and (B1) that the tunneling of an electron-like quasiparticle from S_1 to S_2 is in correspondence with the Andreev bound state having energy ω_0^{21} . Solving Eq. (B5) we can calculate χ_{ee}^{21} and hence \mathcal{T}_{ee}^{21} .

(ii) *Tunneling of a hole (electron)-like quasiparticle from left (right) to right (left)*. Similarly, tunneling of a hole-like quasiparticle from S_1 to S_2 can be mathematically expressed as

$$\begin{aligned} \chi_{hh}^{21} \Psi_{qp}^{h+}[\phi_2] &= \mathbb{T}_B^R (\mathbb{T}^2 + \mathbb{T}^2 \mathbb{R}^2 \mathbb{T}^2 \mathbb{R}^2 \mathbb{T}^2 + \dots) \mathbb{T}_B^L \Psi_{qp}^{h+}[\phi_1] \\ &= \mathbb{T}_B^R \mathbb{T}^2 (\mathbb{I} - \mathbb{R}^2 \mathbb{T}^2 \mathbb{R}^2 \mathbb{T}^2)^{-1} \mathbb{T}_B^L \Psi_{qp}^{h+}[\phi_1]. \end{aligned} \quad (\text{B6})$$

A comparison between Eqs. (B6) and (B3) clearly indicates the fact that the tunneling of a hole-like quasiparticle from S_1 to S_2 is in correspondence with the Andreev bound state having energy ω_0^{12} . Solving Eq. (B6) we can calculate χ_{hh}^{21} and hence \mathcal{T}_{hh}^{21} .

APPENDIX C: SIGNIFICANCE OF THE QUANTITY $(k_e - k_h)L/2$

We have assumed the doping of the junction is sufficiently high, so let us retain the expressions of k_e and k_h up to the first order of ω/μ for quadratic dispersion relation,

$$\begin{aligned} k_e &= \frac{\sqrt{2m}}{\hbar} \sqrt{\mu + \omega} \approx \frac{\sqrt{2m\mu}}{\hbar} \left(1 + \frac{\omega}{2\mu}\right); \\ k_h &= \frac{\sqrt{2m}}{\hbar} \sqrt{\mu - \omega} \approx \frac{\sqrt{2m\mu}}{\hbar} \left(1 - \frac{\omega}{2\mu}\right). \end{aligned} \quad (\text{C1})$$

Now, we shall consider the length of the junction L to be finite compare to the superconducting coherence length $\xi = \hbar\sqrt{2\mu/m}/\Delta_0$ so let $L = x\xi$. Now

$$\begin{aligned} \frac{k_e - k_h}{2} L &\approx \frac{1}{2} \frac{\sqrt{2m\mu}}{\hbar} \left[\left(1 + \frac{\omega}{2\mu}\right) - \left(1 - \frac{\omega}{2\mu}\right) \right] x\xi \\ &\approx \frac{1}{2} \frac{\sqrt{2m\mu}}{\hbar} \frac{\omega}{\mu} \left(x \frac{\hbar}{\Delta_0} \sqrt{\frac{2\mu}{m}} \right) \approx x \frac{\omega}{\Delta_0}. \end{aligned} \quad (\text{C2})$$

Thus, even for large enough doping, the quantity $(k_e - k_h)L/2$ is of the order of ω/Δ_0 , and thus cannot be neglected.

For linear dispersion relation, $k_e = \frac{\mu + \omega}{\hbar v_F}$ and $k_h = \frac{\mu - \omega}{\hbar v_F}$, hence, here also $\frac{k_e - k_h}{2} L \approx x \frac{\omega}{\Delta_0}$.

APPENDIX D: PRESENCE OF A SCATTERER IN THE MIDDLE OF THE JUNCTION

Starting with an initial state $((\Psi_N^{e+}|_{x=-L/2}), (\Psi_N^{e-}|_{x=L/2}))^T$, it will come back to the same state after a electron scattering followed by an Andreev reflection, a hole scattering and another Andreev reflection. For $\omega < \Delta_0$, these matrices all being unitary, it must be

$$\begin{bmatrix} \Psi_N^{e+}|_{x=-L/2} \\ \Psi_N^{e-}|_{x=L/2} \end{bmatrix} = \mathbb{R}_P^A \mathcal{T}_P^h \mathbb{R}_P^A \mathcal{T}_P^e \begin{bmatrix} \Psi_N^{e+}|_{x=-L/2} \\ \Psi_N^{e-}|_{x=L/2} \end{bmatrix} \quad (\text{D1})$$

where we have defined $\mathbb{M}_P = \mathbb{M} \mathbb{T}^P$. Note that, in the absence of barrier, i.e., at $\mathcal{T}^e = \mathcal{T}^h = \mathbb{I}$, all the matrices \mathbb{T}^P , \mathbb{R}^A , \mathcal{T}^e and \mathcal{T}^h are block diagonal and the aforesaid two types of ABS (ω_0^{21} and ω_0^{12}) do not interfere. In presence of barrier, finite backscattering (off-diagonal blocks of \mathcal{T}^e and \mathcal{T}^h) gives rise to the interference between the two types of ABS (ω_0^{21} and ω_0^{12}).

ABS energies, in presence of barrier can be obtained by solving the equation

$$\det(\mathbb{I}_{4 \times 4} - \mathbb{R}_P^A \mathcal{T}_P^h \mathbb{R}_P^A \mathcal{T}_P^e) = 0. \quad (\text{D2})$$

Note that, if we had started with the initial state $((\Psi^{h-}|_{x=L/2}), (\Psi^{h+}|_{x=-L/2}))^T$ then Eq. (D2) would have looked like

$$\det(\mathbb{I}_{4 \times 4} - \mathbb{R}_P^A \mathcal{T}_P^e \mathbb{R}_P^A \mathcal{T}_P^h) = 0. \quad (\text{D3})$$

It turns out, the ABS energies, as obtained from (D2) or (D3) are same.

For energies $\omega > \Delta_0$, we define the following matrices:

$$\mathbb{T}^L = \begin{bmatrix} \mathbb{T}_B^L & 0 \\ 0 & \mathbb{T}_B^L \end{bmatrix} \quad \mathbb{T}_e^R = \begin{bmatrix} \mathbb{T}_B^R & 0 \\ 0 & 0 \end{bmatrix} \quad \mathbb{T}_h^R = \begin{bmatrix} 0 & 0 \\ 0 & \mathbb{T}_B^R \end{bmatrix}.$$

With this, tunneling of a QP from S_1 to S_2 can be understood as follows:

(i) An incident electron-like QP in S_1 $((\Psi_{qp}^{e+}[\phi_1]), (0))^T$ can tunnel into S_2 as an electron-like QP $((\Psi_{qp}^{e+}[\phi_2]), (0))^T$ either directly or by any even number of Andreev reflections whereas tunneling of an electron-like QP from S_1 to S_2 as a hole-like QP $((0), (\Psi_{qp}^{h+}[\phi_2]))^T$ must be mediated by an odd number of Andreev reflections,

$$\begin{aligned} \chi_{ee}^{21} \begin{bmatrix} \Psi_{qp}^{e+}[\phi_2] \\ 0 \end{bmatrix} &= \mathbb{T}_e^R \mathbb{T}^P \mathcal{T}_P^e (\mathbb{B}^e)^{-1} \mathbb{T}^L \begin{bmatrix} \Psi_{qp}^{e+}[\phi_1] \\ 0 \end{bmatrix}, \\ \chi_{he}^{21} \begin{bmatrix} 0 \\ \Psi_{qp}^{h+}[\phi_2] \end{bmatrix} &= \mathbb{T}_h^R \mathbb{T}^P \mathcal{T}_P^h \mathbb{R}_P^A \mathcal{T}_P^e (\mathbb{B}^e)^{-1} \mathbb{T}^L \begin{bmatrix} \Psi_{qp}^{e+}[\phi_1] \\ 0 \end{bmatrix} \end{aligned}$$

where $\mathbb{B}^e = \mathbb{I}_{4 \times 4} - \mathbb{R}_P^A \mathcal{T}_P^h \mathbb{R}_P^A \mathcal{T}_P^e$. Solving above equations we can calculate χ_{ee}^{21} and χ_{he}^{21} and hence we \mathcal{T}_{ee}^{21} and \mathcal{T}_{he}^{21} .

(ii) Similarly, tunneling of a hole-like QP from S_1 $((0), (\Psi_{qp}^{h+}[\phi_1]))^T$ into S_2 as an hole-like QP

$((0), (\Psi_{qp}^{h+}[\phi_2]))^T$ can be mediated directly or by any even number of Andreev reflections whereas tunneling of a hole-like QP from S_1 to S_2 as an electron-like QP $((\Psi_{qp}^{e+}[\phi_2]), (0))^T$ must be mediated by an odd number of Andreev reflections,

$$\begin{aligned}\chi_{hh}^{21} \begin{bmatrix} 0 \\ \Psi_{qp}^{h+}[\phi_2] \end{bmatrix} &= \mathbb{T}_h^R \mathbb{T}^P \mathcal{T}_P^h (\mathbb{B}^h)^{-1} \mathbb{T}^L \begin{bmatrix} 0 \\ \Psi_{qp}^{h+}[\phi_1] \end{bmatrix}, \\ \chi_{eh}^{21} \begin{bmatrix} \Psi_{qp}^{e+}[\phi_2] \\ 0 \end{bmatrix} &= \mathbb{T}_e^R \mathbb{T}^P \mathcal{T}_P^e \mathbb{R}_P^A \mathcal{T}_P^h (\mathbb{B}^h)^{-1} \mathbb{T}^L \begin{bmatrix} 0 \\ \Psi_{qp}^{h+}[\phi_1] \end{bmatrix}\end{aligned}$$

where $\mathbb{B}^h = \mathbb{I}_{4 \times 4} - \mathbb{R}_P^A \mathcal{T}_P^e \mathbb{R}_P^A \mathcal{T}_P^h$. Solving above equations we can calculate \mathcal{T}_{hh}^{21} and \mathcal{T}_{eh}^{21} .

APPENDIX E: MAXIMUM POSSIBLE THERMO-CURRENT COEFFICIENT WITH THE SCATTERER AT THE MIDDLE OF THE JUNCTION

We have used the formalism as discussed in Appendix D to calculate the quantities \mathcal{T}_{ee}^{21} , \mathcal{T}_{he}^{21} , \mathcal{T}_{hh}^{21} , and \mathcal{T}_{eh}^{21} . We have assumed the doping to be high enough so that the quasiparticle momenta $p_i \approx p_F$, where p_F is the Fermi momentum, leading to perfect Andreev reflections at the normal metal-superconductor boundaries but $(p_e - p_h)L/\hbar \neq 0$, within the normal region, due to the finite length of the junction. With

this assumption, different transmission probabilities turns out to be

$$\mathcal{T}_{ee}^{21,\eta} = \frac{2\tau \sinh^2 \alpha (\cosh 2\alpha - \cos[(k_e - k_h)L + \phi_{12}])}{\Omega(\eta)\Omega^*(\eta)}, \quad (\text{E1})$$

$$\mathcal{T}_{hh}^{21,\eta} = \frac{2\tau \sinh^2 \alpha (\cosh 2\alpha - \cos[(k_e - k_h)L - \phi_{12}])}{\Omega(\eta)\Omega^*(\eta)}, \quad (\text{E2})$$

$$\mathcal{T}_{he}^{21,\eta} = \frac{2\tau(1-\tau) \sinh^2 \alpha (1 - \eta \cos \phi_{12})}{\Omega(\eta)\Omega^*(\eta)} = \mathcal{T}_{eh}^{21,\eta}, \quad (\text{E3})$$

where $\Omega(\eta) = (1 - \eta \cos[(k_e - k_h)L + 2i\alpha]) - \tau(1 - \eta \cos \phi_{12})$, $\alpha = \text{arccosh}(\omega/\Delta_0)$, τ is the transmission probability of the scatterer placed at the middle of the junction and $\eta = \pm 1$ for s -wave and p -wave superconductivity respectively.

We have used the above expressions and Eq. (4) of the main text to calculate the thermocurrent coefficient of a JJ with either s -wave or p -wave superconductivity. Now for a fixed value of the length of the junction L and for a fixed value of the transmission probability τ of the scatterer at the middle of the junction, we have calculated the thermocurrent coefficient for different values of the superconducting phase different ϕ_{12} within $0 \leq \phi_{12} \leq 2\pi$ in steps of 0.01π and we recorded only the maximum value κ_e^{21} in this process.

Now, we have varied τ within $1 \geq \tau \geq 0$ in steps of 0.01 and L within $0 \leq L \leq 5\xi$ in steps of 0.01ξ . For each set of values of $\{L, \tau\}$ we have repeated the previous process to obtain the maximum possible value of κ_e^{21} . Lastly we have plotted this maximum possible value of κ_e^{21} , scanned over ϕ_{12} , as a function of L and τ . This is shown in Fig. 6.

-
- [1] U. Sivan and Y. Imry, *Phys. Rev. B* **33**, 551 (1986).
[2] A. A. M. Staring, L. W. Molenkamp, B. W. Alphenaar, H. van Houten, O. J. A. Buyk, M. A. A. Mabeoone, C. W. J. Beenakker, and C. T. Foxon, *Europhys. Lett.* **22**, 57 (1993).
[3] S. Möller, H. Buhmann, S. F. Godijn, and L. W. Molenkamp, *Phys. Rev. Lett.* **81**, 5197 (1998).
[4] R. Scheibner, H. Buhmann, D. Reuter, M. N. Kiselev, and L. W. Molenkamp, *Phys. Rev. Lett.* **95**, 176602 (2005).
[5] B. Ludoph and J. M. van Ruitenbeek, *Phys. Rev. B* **59**, 12290 (1999).
[6] P. Reddy, S.-Y. Jang, R. A. Segalman, and A. Majumdar, *Science* **315**, 1568 (2007).
[7] J. R. Widawsky, P. Darancet, J. B. Neaton, and L. Venkataraman, *Nano Lett.* **12**, 354 (2012).
[8] H. Thierschmann, R. Sánchez, B. Sothmann, F. Arnold, C. Heyn, W. Hansen, H. Buhmann, and L. W. Molenkamp, *Nat. Nanotechnol.* **10**, 854 (2015).
[9] A. Shakouri, *Annu. Rev. Mater. Res.* **41**, 399 (2011).
[10] R. Sánchez and M. Büttiker, *Phys. Rev. B* **83**, 085428 (2011).
[11] C. W. J. Beenakker and A. A. M. Staring, *Phys. Rev. B* **46**, 9667 (1992).
[12] O. Entin-Wohlman, Y. Imry, and A. Aharony, *Phys. Rev. B* **82**, 115314 (2010).
[13] D. Sánchez and L. Serra, *Phys. Rev. B* **84**, 201307(R) (2011).
[14] A. N. Jordan, B. Sothmann, R. Sánchez, and M. Büttiker, *Phys. Rev. B* **87**, 075312 (2013).
[15] K. Brandner, K. Saito, and U. Seifert, *Phys. Rev. Lett.* **110**, 070603 (2013).
[16] S. Kolenda, M. J. Wolf, and D. Beckmann, *Phys. Rev. Lett.* **116**, 097001 (2016).
[17] S. Kolenda, C. Sürgers, G. Fischer, and D. Beckmann, *Phys. Rev. B* **95**, 224505 (2017).
[18] S. Shimizu, J. Shiogai, N. Takemori, S. Sakai, H. Ikeda, R. Arita, T. Nojima, A. Tsukazaki, and Y. Iwasa, *Nat. Commun.* **10**, 825 (2019).
[19] Z. B. Tan, A. Laitinen, N. S. Kirsanov, A. Galda, V. M. Vinokur, M. Haque, A. Savin, D. S. Golubev, G. B. Lesovik, and P. J. Hakonen, *Nat. Commun.* **12**, 138 (2021).
[20] A. Fornieri and F. Giazotto, *Nat. Nanotechnol.* **12**, 944 (2017).
[21] F. Giazotto, T. T. Heikkilä, A. Luukanen, A. M. Savin, and J. P. Pekola, *Rev. Mod. Phys.* **78**, 217 (2006).
[22] V. L. Ginzburg, *Zh. Eksp. Teor. Fiz.* **14** 177 (1944) [*J. Phys. USSR* **8**, 148 (1944)].
[23] V. L. Ginzburg, *Rev. Mod. Phys.* **76**, 981 (2004).
[24] V. L. Ginzburg, *Supercond. Sci. Technol.* **4**, S1 (1991).
[25] V. Ginzburg and G. Zharkov, *Physica C* **235-240**, 3129 (1994).
[26] D. C. Marinescu and A. W. Overhauser, *Phys. Rev. B* **55**, 11637 (1997).

- [27] Yu. M. Galperin, V. L. Gurevich, and V. I. Kozub, *Zh. Eksp. Teor. Fiz.* **66**, 1387 (1974) [*Sov. Phys.-JETP* **39**, 680 (1974)]; A. G. Aronov, *Zh. Eksp. Teor. Fiz.* **67**, 178 (1974) [*Sov. Phys.-JETP* **40**, 90 (1975)].
- [28] Y. M. Galperin, V. L. Gurevich, V. I. Kozub, and A. L. Shelankov, *Phys. Rev. B* **65**, 064531 (2002).
- [29] P. Virtanen and T. T. Heikkilä, *Appl. Phys. A* **89**, 625 (2007).
- [30] C. M. Falco and J. C. Garland, Thermoelectric effects in superconductors, in *Nonequilibrium Superconductivity, Phonons, and Kapitza Boundaries*, NATO Advanced Study Institutes Series, edited by K. E. Gray (Springer, Boston, MA, 1981), Vol. 65, pp. 521–540.
- [31] G. Borelius, W. H. Keesom, C. H. Johansson, and J. O. Linde, *Proc. Koninkl. Ned. Akad. Wetenschap*, Vol. 34 (Comm. Kamerlingh Onnes Lab, Leiden, 1931), p. 1365.
- [32] E. Burton, F. Tarr, and J. Wilhelm, *Nature (London)* **136**, 141 (1935).
- [33] W. Keesom and C. Matthijs, *Physica* **5**, 437 (1938).
- [34] H. B. G. Casimir and A. Rademakers, *Physica* **13**, 33 (1947).
- [35] G. T. Pullan, *Proc. R. Soc. London A* **217**, 280 (1953).
- [36] D. J. Van Harlingen, D. F. Heidel, and J. C. Garland, *Phys. Rev. B* **21**, 1842 (1980).
- [37] M. V. Kartsovnik, V. V. Ryazanov, and V. V. Shmidt, *JETP Lett.* **33**:7 (1981).
- [38] A. Fornieri, C. Blanc, R. Bosisio, S. D’ambrosio, and F. Giazotto, *Nat. Nanotechnol.* **11**, 258 (2016).
- [39] C. D. Shelly, E. A. Matrozova, and V. T. Petrashov, *Sci. Adv.* **2**, e1501250 (2016).
- [40] B. D. Josephson, *Phys. Lett.* **1**, 251 (1962).
- [41] G. D. Guttman, B. Nathanson, E. Ben-Jacob, and D. J. Bergman, *Phys. Rev. B* **55**, 12691 (1997).
- [42] S. S. Pershoguba and L. I. Glazman, *Phys. Rev. B* **99**, 134514 (2019).
- [43] S. Hart, H. Ren, T. Wagner, P. Leubner, M. Mühlbauer, C. Brüne, H. Buhmann, L. W. Molenkamp, and A. Yacoby, *Nat. Phys.* **10**, 638 (2014).
- [44] G. Marchegiani, A. Braggio, and F. Giazotto, *Phys. Rev. Lett.* **124**, 106801 (2020).
- [45] D. Sánchez and R. López, *C. R. Phys.* **17**, 1060 (2016).
- [46] M. Banerjee, M. Heiblum, A. Rosenblatt, Y. Oreg, D. E. Feldman, A. Stern, and V. Umansky, *Nature (London)* **545**, 75 (2017).
- [47] D. Gresta, M. Real, and L. Arrachea, *Phys. Rev. Lett.* **123**, 186801 (2019).
- [48] G. Marchegiani, A. Braggio, and F. Giazotto, *Appl. Phys. Lett.* **117**, 212601 (2020).
- [49] G. Blasi, F. Taddei, L. Arrachea, M. Carrega, and A. Braggio, *Phys. Rev. Lett.* **124**, 227701 (2020).
- [50] G. Blasi, F. Taddei, L. Arrachea, M. Carrega, and A. Braggio, *Phys. Rev. B* **103**, 235434 (2021).
- [51] G. Blasi, F. Taddei, L. Arrachea, M. Carrega, and A. Braggio, *Phys. Rev. B* **102**, 241302(R) (2020).
- [52] M. Li and G. Chen, *MRS Bull.* **45**, 348 (2020).
- [53] L. Fu and C. L. Kane, *Phys. Rev. B* **79**, 161408(R) (2009).
- [54] L. Fu and C. L. Kane, *Phys. Rev. Lett.* **100**, 096407 (2008).
- [55] A. Calzona and B. Trauzettel, *Phys. Rev. Research* **1**, 033212 (2019).
- [56] A. L. Fetter and J. D. Walecka, *Quantum Theory of Many-Particle Systems*, Dover Books on Physics (Dover Publications, New York, 2012).
- [57] G. Annunziata, H. Enoksen, J. Linder, M. Cuoco, C. Noce, and A. Sudbø, *Phys. Rev. B* **83**, 144520 (2011).
- [58] J. Wang, Y. Zhao, H.-H. Liao, S. Priya, and S. T. Huxtable, *Meas. Sci. Technol.* **30**, 075901 (2019).
- [59] B. Sothmann and E. M. Hankiewicz, *Phys. Rev. B* **94**, 081407 (2016).
- [60] A. Kundu, S. Rao, and A. Saha, *Phys. Rev. B* **82**, 155441 (2010).
- [61] T. S. Tinyukova and Y. P. Chuburin, *Izv. IMI UdGU* **54**, 55 (2019).